Increased CO_2 Fixation Enables High Carbon-Yield Production of the Acrylic Acid Precursor 3-Hydroxypropionic Acid in Yeast

Zihe Liu

zihe@buct.edu.cn

Beijing university of chemical technology

Ning Qin

Beijing university of chemical technology

Lingyun Li

Beijing university of chemical technology

Xiaozhen Wan

Beijing university of chemical technology

Xu Ji

Beijing university of chemical technology

Yu Chen

Shenzhen Institute of Advanced Technology, Chinese Academy of Sciences https://orcid.org/0000-0003-3326-9068

Chaokun Li

University of Helsinki

Ping Liu

Beijing university of chemical technology

Yijie Zhang

Beijing university of chemical technology

Weijie Yang

Beijing university of chemical technology

Junfeng Jang

Chinese Academy of Sciences

Jianye Xia

Chinese Academy of Sciences

Shuobo Shi

Beijing University of Chemical Technology https://orcid.org/0000-0002-0261-3105

Tianwei Tan

Beijing university of chemical technology

Jens Nielsen
Chalmers University of Technology
Yun Chen
Chalmers University of Technology

Article

Keywords: bicarbonate, 3-hydroxypropionic acid, high carbon-yield production, Espb6, Malonyl-CoA reductase

Posted Date: September 15th, 2023

DOI: https://doi.org/10.21203/rs.3.rs-3278694/v1

Additional Declarations: There is **NO** Competing Interest.

Version of Record: A version of this preprint was published at Nature Communications on February 21st, 2024. See the published version at https://doi.org/10.1038/s41467-024-45557-9.

Abstract

CO_2 fixation plays a key role to make biobased production cost competitive. Here, we used 3-hydroxypropionic acid (3-HP) to showcase how CO_2 fixation enabled approaching theoretical-yield production. Using genome-scale metabolic models to calculate the production envelope, we demonstrated that the provision of bicarbonate, formed from CO_2, sealed previous attempts for high yield production of 3-HP. We thus developed multiple strategies for bicarbonate uptake, including the identification of Sul1 as a bicarbonate transporter, domain swapping and engineering of malonyl-CoA reductase, identification of Esbp6 as a 3-HP exporter, and deletion of Uga1 to prevent 3-HP degradation. The combined rational engineering increased 3-HP production from 0.15 g/L to 11.25 g/L in shake-flask using 20 g/L glucose, approaching the maximum theoretical yield with concurrent biomass formation. The engineered yeast forms the basis for commercialization of bio-acrylic acid, while our CO_2 fixation strategies pave the way for CO_2 being used as the sole carbon source.

Introduction

Biobased chemical[1] and biofuel[2] production as replacement of petroleum-based production could assist in mitigating green-house gas emissions while establishing sustainable production[3]. However, these biobased productions also result in emissions of the greenhouse gas CO_2, and fixing emitted CO_2 into products is therefore of great interest[4], in particular as this may also result in higher carbon-yields and therefore improves process economics.

Intracellular inorganic carbon exists in four forms: dissolved CO_2, carbonic acid, bicarbonate, and carbonate[5], that could be interconverted based on the pH and salinity. It has been reported that compared with 5% CO_2 supply, 10% CO_2 could increase itaconic acid production by two-fold in yeast[6]. At pH 7.4 and 20°C, the concentration of CO_2 in equilibrium with the gaseous state is only 0.012 mM, whereas the concentration of bicarbonate in equilibrium with air is 0.26 mM[7]. Since the pH in the cytoplasm is approximately neutral[8], inorganic carbon mainly exists in the form of bicarbonate[9], which means increasing intracellular bicarbonate concentrations could be more appealing than enhancing the higher CO_2 partial pressure. Bicarbonate can be captured by native carboxylation reactions, of which the acetyl-CoA carboxylation catalysed by acetyl-CoA carboxylase Acc1 is known to carry a high flux in yeast. The generated malonyl-CoA can be transformed into 3-hydroxypropionic acid (3-HP), which represents a valuable chemical intermediate. Efficient capture of CO_2 into 3-HP can improve the carbon yield in its production, and this step is also crucial in the native CO_2 fixation pathway 3-hydroxypropionate/4-hydroxybutyrate (HP/HB) cycle[10, 11].

3-HP holds a significant position as the potentially third-largest biobased platform compound, with an estimated potential annual market size of USD 10 billion[12, 13]. One of the key reasons behind its prominence is its ease of dehydration into acrylate, a crucial component used in the production of

synthetic polymers like super-absorbents applied in disposable diapers[14]. The production of 3-HP has thus garnered considerable attention, but the major hurdle remains the low yield of 3-HP on the substrate, posing a significant challenge to establish an industrial scale process[15]. A comprehensive analysis of 3-HP production in yeast reveals that the best yield achieved thus far in terms of the 3-HP to substrate (glucose) ratio is approximately 0.31g/g[16], which corresponds to only 39.7% of the maximum theoretical yield[15]. This falls short of the commercial requirement for 3-HP to acrylate production, which highlights the current limitations in 3-HP production and underscores the need for significant improvements in yield to meet the demands of the industry.

In this study we found, using metabolic modelling, that the production envelope in previous attempts to produce 3-HP has been sealed by the availability of bicarbonate. We therefore engineered yeast to break this seal and hereby achieved high carbon yield production of 3-HP. This was achieved through employing multiple strategies to increase the accessible bicarbonate, minimize native CO_2 release, as well as by avoiding carbon waste. Hereby we achieved a record high yield of 0.5625 g/g (89.3% of the theoretical yield of 3-HP with biomass generation). Furthermore, the high titer of 3-HP obtained through a microbial fermentation could easily be transformed to acrylate with a yield of 100%.

Results

Limited provision of bicarbonate seals 3-HP production

The production envelope of 3-HP via the malonyl-CoA reductase pathway was calculated using the Yeast8 model[17], and this was used to analyse the carbon flux and identify limiting factors for 3-HP production. Contrary to the general belief that the precursors of acetyl-CoA and malonyl-CoA, as well as the redox cofactors and ATP were the key requirements for 3-HP production, our analysis suggested that a high flux of bicarbonate (Fig. 1a) was crucial for efficient 3-HP production, i.e. the flux of bicarbonate needed to be 1.562 times higher than that of the substrate (glucose) to achieve the maximum 3-HP production (Fig. 1a). Unfortunately, such a flux of bicarbonate is unattainable within the native metabolism, even if we assume that bicarbonate can be freely converted from CO_2. The cellular metabolism is simply incapable of providing a sufficient amount of CO_2 to generate the required bicarbonate for 3-HP production[18], regardless of the metabolic state—be it respiration (efficient CO_2 generation state) or fermentation (non-efficient CO_2 generation state) (Fig. 1a). Moreover, if we consider that the CO_2 generated is in a gaseous state intracellularly, it will promptly leave the liquid phase, and the carboxylation process by Acc1 necessitates the presence of bicarbonate dissolved in water (Fig. 1b). This further exacerbates the deficiency of bicarbonate. Specifically, in the native metabolic context, the limited flux of bicarbonate significantly reduced the theoretical maximum yield of 3-HP from 0.781 to approximately 0.440 g/g (fermentation state)-0.490 g/g (respiration state) (Fig. 1a). This result indicated that the availability of bicarbonate is the primary bottleneck for 3-HP production, effectively sealing all previous attempts at metabolic flux rewiring in this production envelope boundary. To address this issue,

it is imperative to ensure an ample supply of bicarbonate for Acc1 carboxylation while minimizing CO_2 loss during acetyl-CoA and energy generation.

Carbon conserved loop from glucose to 3-HP

We started by establishing a "carbon conserved loop" that effectively recycled the lost carbon to maximize a high carbon-yield for the production of 3-HP (Fig. 1b). The split bi-functional enzyme MCR from *Chloroflexus aurantiacus* was used for 3-HP production, as it can catalyse the conversion of malonyl-CoA to malonic semialdehyde (MSA) via the MCR-C domain and then to 3-HP via the MCR-N domain (Fig. 1b)[19]. Integration of the split MCR into the chromosome together with *ACC1* overexpression resulted in a 3-HP titer of 0.15 g/L in the QLW1 strain (Fig. 1c). Next, to reduce the CO_2 release while producing acetyl-CoA, we integrated the phosphoketolase (PK) pathway reported in our previous study[20], and enhanced 3-HP production to 0.39 g/L. Further, to release Acc1 from post-translational regulation, we introduced two site mutations, S659A and S1157A, which prevent phosphorylation of Acc1 by Snf1, thereby activating Acc1 activity[21]. It then resulted in an increased 3-HP titer to 0.65 g/L in the QLW3 strain (Fig. 1c).

To achieve a higher flux through the PK pathway, extensive genotype modifications were reported to redirect carbon flux from glycolysis to the oxidative pentose phosphate (oxPP pathway)[20]. We instead turn to transcription factors (TFs) to investigate whether a single gene modification could achieve the overall carbon flux rewiring. Stb5 is a TF and an NADPH regulator[22] that represses the expression of *PGI1*, coding the rate-limiting reaction of the whole glycolysis at glucose-6-P to rewire the flux from glycolysis to the oxPP pathway[23]. Stb5 has been used to redirect the carbon flux for the production of protopanaxadiol in yeast[24]. We thus overexpressed *STB5* with the *TEF1* promoter. However, the growth of the strain was significantly inhibited (Fig. S1). qPCR results indicated that the strength of the *TEF1* promoter was around 10-fold higher than that of the native *STB5* promoter (Fig. 1d), which may have been too strong for regulating the TF expression in the cell. Thus, we placed the TATA box adjacent to the core promoter of *TEF1*[25] (Fig. 1d) and constructed an artificial promoter to replace the native promoter of *STB5*, and qPCR results showed that its strength was around 2.5-fold greater than that of the native *STB5* promoter (Fig. 1d). Indeed, the strain with this artificial promoter-controlled Stb5 enhanced 3-HP production to 0.74 g/L (Fig. 1c).

Meanwhile, we tried to employ carbonic anhydrase and a bicarbonate transporter to enhance the intracellular bicarbonate content for the production of 3-HP (Fig. 1e). This CO_2 concentrating system has successfully increased the production of succinate in *E. coli*[26, 27]. Overexpression of *NCE103*, the native carbonic anhydrase in yeast[28], could also improve 3-HP production to 0.7 g/L in QLW6 (Fig. 1f). Considered the flux restricted from CO_2 (Fig. 1a), we next tried to find a native bicarbonate transporter in yeast.

Bicarbonate diffuses poorly into the cell[26], and therefore requires SLC4 and SLC26 as two kinds of anion transporters to assist the active transport process[29]. Bor1, a boron efflux transporter of the plasma membrane, can also bind bicarbonate, belonging to the SLC4 family (Fig. 1g)[30], whereas no bicarbonate transporter from the SLC26 family has been reported in yeast[31]. To identify potential bicarbonate transporters, we performed a phylogenetic analysis of key species of the SLC4 and SLC26 families (Fig. 1g). We identified Sul1/2, which were previously regarded as sulphate permeases[32]. Bor1 is an efflux transporter, while Sul1/2 are influx transporters. Thus, we overexpressed *SUL1*, *SUL2* and deleted *BOR1*, respectively. Hereby the 3-HP titer increased to 0.83 g/L in *SUL1* overexpressing yeast, which was a 27.7% improvement over the control strain (Fig. 1f, QLW8). Meanwhile, the final OD_{600} of this strain also increased from 6.97 to 7.65, which was 9.8% higher than the control strain (Fig. S2). These results highlight the importance of bicarbonate transporters for efficient carbon fixation.

Next, we intended to combine strategies before to close this “carbon conservation loop”, yet the 3-HP production in the QLW10 strain dropped to 0.31 g/L, which was even lower than that of the control strains QLW5 and QLW8 (Fig. 1h). Analysis of extracellular metabolites in the medium revealed the presence of 0.37 g/L of oxaloacetate (Fig. S3), which is uncommon as there was usually no oxaloacetate accumulated in the medium. We speculated that the increased intracellular bicarbonate content also improved other bicarbonate utilizing reactions, such as the carboxylation of pyruvate to oxaloacetate catalysed by Pyc1 and Pyc2, and tried various strategies to decrease the accumulation of oxaloacetate (Fig. 1i). Yet, the deletion of *CIT2* that encoded the key gene of the glyoxylate cycle should prevent the accumulation of oxaloacetate only slightly recovered 3-HP titer (Fig. 1h, QLW11), with acetate accumulated instead. We next focused on enhancing the utilization of oxaloacetate by the TCA cycle, which could generate more ATP for the carboxylation reaction catalysed by Acc1. Firstly, we overexpressed *CIT1*, and improved 3-HP production to 0.44 g/L (Fig. 1h, QLW12). Meanwhile, we tested $Cit1^{S462A}$ enabling the enzyme to defer phosphorylation regulation[33], and increased 3-HP production to 0.45 g/L (Fig. 1h, QLW13). We also overexpressed Ptc6 and Ptc7 which could selectively dephosphorylate mitochondrial proteins, especially the Ptc7 that could dephosphorylate Cit1 and enhance yeast respiration[34]. Indeed, overexpression of *PTC7* in the QLW15 strain could not only recover but further increase the production of 3-HP to 1.18 g/L (Fig. 1h). Next, we overexpressed Yhm2, an oxaloacetate transporter in the mitochondrial membrane, and Idp2 that could provide more NADPH for the production of fatty acids[35], and increased 3-HP production to 1.34 g/L, an 81.1% and 60.9% improvement over the control (Fig. 1h, QLW5 and QLW8).

Improved conversion of malonyl-CoA to 3-HP

To provide enough malonyl-CoA for 3-HP production, another copy of $ACC1^{S659A\ S1157A}$ with *TEF1* promoter was integrated into the chromosome, but the growth of the strain was strongly reduced. The intracellular malonyl-CoA level is strictly regulated by the AMPK[36] pathway and a high concentration of malonyl-CoA was found to be toxic for the cell[37]. This result suggested that the elevated malonyl-CoA

concentration being beyond the range the cell could handle[38]. Therefore, we focused on more efficient conversion of malonyl-CoA into 3-HP.

We started by expressing MCR-N and MCR-C in different combinations, and expressing the MCR-N domain and MCR-C$^{N941V\ K1107W\ S1115R}$ domain[16, 19] using a higher copy number plasmid increased 3-HP production to 4.12 g/L in QLW23 (Fig. 2a and 2b). Currently, there is no crystal structure of MCR from *C. aurantiacus* and only crystal structures of the MCR-N domain and the MCR-C domain from *Porphyrobacter dokdonensis* have been published[39]. Using SWISS-MODEL, we generated a homologous model of MCR from *C. aurantiacus* using the known structures of the MCR-N domain (PDB: 6k8v) and MCR-C domain (PDB: 6k8s) from *P. dokdonensis* (Fig. 2c) as template. Next, we analysed the structure and noticed that the MCR-N domain could be separated into two short-chain dehydrogenase/reductase (SDR) domains: SDR domain 1 (MCR-N domain/SDR1, M1–L284) and SDR domain 2 (MCR-N domain/SDR2, P285–I550). The MCR structure revealed that the cofactor and substrate only bind to the SDR1 domain, indicating that enzyme catalysis cannot occur at the SDR2 of the MCR-N domain[39]. Yet, to increase the catalytic efficiency of the MCR-N domain, we deleted the MCR-N-SDR2 domain and found that the production of 3-HP had a strong decrease (Fig. 2d, QLW24). This result may be because even though the MCR-N-SDR2 domain has no catalytic function it may help the MCR-N-SDR1 domain to maintain its proper structure. To find a more efficient domain converting MSA to 3-HP, we performed domain swapping using SDRs from different species and obtained the most efficient malonyl-CoA reductase reported. Specially, we identified new MCR-N-SDR1 domains such as Ora1 (reported as the serine dehydrogenase) from *S. cerevisiae*, and ydfG (reported as the $NADP^+$-dependent dehydrogenase with broad substrate specificity on 3-hydroxy acids) from *E. coli* for the active analysis (Fig. 2c). The Ora1 and ydfG exhibited 26.1% and 28.5% improvements, producing 5.2 g/L and 5.3 g/L 3-HP, respectively (Fig. 2d). Neither codon optimization or the application of a protein linker[40] could further improve the production of 3-HP (Fig. 2d). The finding that common cell factories such as *S. cerevisiae* and *E. coli* possess native enzymes catalysing malonic semialdehyde to 3-HP could potentially explain why adjusting the expression the of MCR-N domain and MCR-C domain was always irregular and been impute into an ambiguity explainations[19, 41].

Meanwhile, since malonyl-CoA was also utilized for fatty acid synthesis in the cell[42], we tried to reduce the generation of fatty acids to increase the production of 3-HP (Fig. 2e). Specially, we used the *COX9* promoter, which is a weaker promoter than the native *FAS1* promoter, and *HXT1* promoter, which is repressed by glucose, to control the expression of *FAS1*, respectively[43] (Fig. 2f). Using this approach, we were able to increase the titer of 3-HP to 5.87 g/L (Fig. 2f, QLW30). Meanwhile, we also up-regulated the *β*-oxidation pathway to decompose fatty acids back to NADPH and acetyl-CoA for 3-HP production (Fig. 2e). The resulting QLW34 strain overexpressing *POX2* with *PGK1* promoter improved 3-HP production to 5.92 g/L. Similarly, the QLW33 strain overexpressing *POX1* with *CCW12* promoter also improved the titer to 5.8 g/L (Fig. 2f). We thus combined these strategies, yet we did not observe a superimposed effect, with the 3-HP production in QLW36 fluctuated around 6 g/L (Fig. 2f). To verify the repression of lipid synthesis, we used Nile red that specifically binds to neutral lipids to characterize the

yeast. The results showed a significant reduction in the size and number of lipid droplets in the QLW36 strain (Fig. 2g). These results indicated a successful rewiring of the carbon flux away from fatty acids. That the titer of 3-HP could not be significantly increased may be because of other bottlenecks in the metabolism.

The increased 3-HP tolerance and the identification of a permease for transport of 3-HP

The 3-HP transport and toxicity represent a new bottleneck for further improving 3-HP production in the QLW36 strain. Our experiments showed that after 72 hours of fermentation with 5.5-6 g/L of 3-HP generated (strains QLW30 to QLW36), the pH of the medium dropped below 4. The pKa value of 3-HP is 4.51, and under this pH value, it remains predominantly undissociated in the medium (Fig. 3a). Free undissociated 3-HP can easily penetrate the cell membrane through diffusion and then release protons to become anions in the cytoplasm where the pH is around neutral[8]. The charged nature of the anion cannot diffuse back out of the cell, resulting in its accumulation in the cytosol that could cause intracellular acidification, which is toxic for the cell[44]. The proton and anion must be pumped out of the cell, and this process is ATP-dependent through the H^+-ATPase and ATP-binding cassette (ABC) pumps[44]. This process consumes a large amount of ATP and can result in ATP depletion, leading to a decrease in the overall 3-HP yield.

We started by testing mutations to improve yeast tolerance of 3-HP (Fig. 3b). For example, the Sfa1 bifunctional alcohol dehydrogenase and the $Sfa1^{C276S}$ mutation have been reported to improve 3-HP tolerance in *S. cerevisiae*[45]. Trk1, a component of the Trk1-Trk2 potassium transport system, was reported to improve yeast tolerance to propionate by increasing potassium influx through the $Trk1^{A1169E}$ mutation[46]. Yet, these two mutations could not increase the production of 3-HP neither (Fig. 3b). Moreover, lactate (pKa 3.86) and 3-HP (pKa 4.51) are structural isomers that have been found to exhibit the same degree of growth inhibition at the same undissociated free acid concentration[47, 48]. This indicated that the mutation involved in the tolerance of lactate may have the potential for improving the 3-HP tolerance. The deletion of the Ssb1 ribosome-associated chaperone was reported to improve yeast tolerance to lactate[49]. The deletion of *GSF2* could increase lactate production by releasing the Crabtree effect of yeast[50], leading to upregulation of gene expression involved in respiration, which has a higher ATP yield than fermentation and is crucial to organic acid production[51]. Deletion of *ERF2*, a subunit of a palmitoyltransferase, could increase lactate production but not lactate tolerance in yeast[52]. Deletion of *SAM2*, which catalyses the synthesis of the cellular cofactor S-adenosylmethionine involved in phospholipid biosynthesis and membrane remodelling during acid stress, was also reported to increase lactate production in yeast[53]. Furthermore, the $Sur1^{I245S}$ mutation or the overexpression could increase lactate tolerance and production. Indeed, the results of this study demonstrated that the deletion of *GSF2, ERF2*, and deletion of *SAM2* significantly improved the production of 3-HP, with the production levels reaching 6.45 g/L, 6.32 g/L, and 6.35 g/L respectively (Fig. 3b).

So far, no 3-HP exporter has been reported. Based on the fact that lactate and 3-HP are structural isomers, we next turned to the identification of new 3-HP exporters based on previous lactate reports. Plasma membrane ABC transporter Pdr12, which could transport carboxylic acids with an aliphatic chain ranging from one to seven[54] and the plasma membrane. P2-type H^+-ATPase Pma1[55], which controls the intracellular pH, have been reported to impact lactate stress tolerance in yeast[56]. The overexpression of *ESBP6*, a protein with similarity to monocarboxylate permeases, was reported to significantly improved lactate resistance and production in *S. cerevisiae*[57]. Meanwhile, the deletion of Jen1, the monocarboxylate/proton symporter of the plasma membrane of lactate[58], could increase the production of lactate in yeast[59–61]. Indeed, the overexpression of *ESBP6* significantly improved the production of 3-HP, with the production levels reaching 6.39 g/L (Fig. 3b). To verify the mechanism by which Esbp6 improved 3-HP production, *ESBP6* was overexpressed in the wild type (WT) strain, and could significantly increase cell tolerance compared with WT in a medium containing 50 g/L 3-HP with pH 3.5 (buffered with potassium citrate), while the deletion of *ESBP6* almost completely abolished growth in this medium (Fig. 3c). These results indicated that Esbp6 could help exporting 3-HP out of the cell, thereby increasing the tolerance of yeast and improving 3-HP production. To our knowledge, this was the first exporter of 3-HP reported. Notably, combining the overexpression of *ESBP6* with the deletion of *GSF2* improved 3-HP production to 7.1 g/L in strain QLW50 (Fig. 3b).

The conserved bicarbonate pool for 3-HP production

There are mainly three enzymes utilizing bicarbonate in yeast (Fig. 1i): Acc1 fixes bicarbonate with acetyl-CoA to form malonyl-CoA, Pyc1/2 utilizes bicarbonate to transform pyruvate into oxaloacetate, Cpa1/2 utilizes bicarbonate to generate carbamoyl-phosphate[62], and then to the pyrimidine ring and arginine (Fig. 4a). It has been demonstrated that bicarbonate limitation in the cytoplasm could restricted *de novo* nucleotide synthesis, which inhibits growth of cancer cells (the Weinberg effect)[63]. This enlightens the potential competition for bicarbonate between the *de novo* synthesis of the pyrimidine ring and malonyl-CoA may reduce 3-HP production (Fig. 4a). The plasmid used to express MCR-C and ydfG had a high copy number with a *URA3* marker. This means that the strain with this plasmid will have a stronger expression of *URA3*, a key step in pyrimidine ring synthesis, leading to the potential competition with Acc1 for bicarbonate. To conserve bicarbonate to 3-HP production, we replaced the *URA3* marker with the *HIS3* marker that is not involve in the bicarbonate metabolism (Fig. 4a)[64]. Indeed, the *HIS3* marker plasmid significantly enhanced 3-HP production from 7.1 g/L to 8.22 g/L (Fig. 4b), while the qPCR result only showed a moderate decrease in the plasmid copy number upon the change in the marker gene (Fig. S4). To demonstrate the improvement of 3-HP production by auxotrophic marker swapping was caused by the decrease in the competition of bicarbonate for the *de novo* uracil synthesis, we added isotope labelled $NaH^{13}CO_3$ to the medium and tested the M + 1 present of uracil in strains with different auxotrophic-marker plasmids. Indeed, consistent with the significantly increased 3-HP production, the M + 1 presence of uracil was significantly decreased in the QLW53 strain (Fig. 4b and 4c). These results confirmed that the auxotrophic marker swapping increased the 3-HP production by releasing the 3-HP generation from the bicarbonate competition with the *de novo* uracil synthesis (Fig. 4c). Different

auxotrophs have been shown to impact yeast metabolism[65], which can affect the production of fatty acids[66]. Yet, the mechanisms behind this impact are not fully understood[66]. Here, we demonstrated that the distinct bicarbonate metabolic backgrounds of these auxotrophs turbulent translational and metabolic capacities of yeast[67], thereby increasing the production of 3-HP.

The results of the enhanced 3-HP production with the *HIS3* marker plasmid suggested that cytoplasmic bicarbonate generated from dissolved CO_2 could be limited due to its low solubility. To provide enough bicarbonate for malonyl-CoA generation, we supplemented the medium with 75 mM calcium carbonate, which further enhanced 3-HP production from 8.22 g/L to 9.12 g/L (Fig. 4d). To test whether the increase in 3-HP production was due to the addition of bicarbonate rather than pH buffering, we conducted a production of 3-HP experiment with 2-(*N*-morpholino) ethanesulfonic acid (MES) that could buffer the pH to the same level as calcium carbonate did. The results showed that the titer of the fermentation with MES buffering was only 8.16 g/L, which was not significantly different from the control (Fig. 4d). A similar strategy has been utilized to increase succinate production in industry, but the real reason was not indicated[68, 69]. Here by model calculation and experiment demonstration, we suggested that it is because the limited intracellular CO_2 concentration as well as the thermodynamic and kinetic favouring of the bicarbonate fixation reaction that increased the production.

The inositol phosphate mechanism application provides more ATP for 3-HP production

The positive effect on 3-HP production by deleting *GSF2* indicated that the energy was crucial for the 3-HP yield. If we consider the energy demand for 3-HP transmembrane during production, this ATP deficiency would be worse. To meet the ATP need, we thus selected different strategies to provide more ATP for 3-HP production. *S. cerevisiae* has the Crabtree effect, which produces an excess amount of ethanol in high concentrations of glucose and reduces energy efficiency[70, 71]. Moreover, the P/O ratio of *S. cerevisiae* is around 1, which indicates that one mole of glucose could only generate approximately 16 moles of ATP (oxidation phosphorylation plus substrate phosphorylation)[72]. Thus, rebalancing central metabolism and enhancing the ATP yield from glucose could be important.

When glucose is transformed in the cell, it is first phosphorylated by Hxk2 and cannot be transformed back to the extracellular environment[73] (Fig. 5a). Deleting *HXK2* can reduce the glucose consumption rate, which could release the Crabtree effect to get a higher ATP yield[74]. Similarly, Mth1 is involved in the glucose signalling pathway, and its active form $Mth1^{\Delta 231}$ acts as a transcription factor to repress hexose transporters (Fig. 5a), that ultimately restricts the Crabtree effect and derepress respiration[74]. Meanwhile, the mutation of $Med2^{*432Y}$, which is the tail module of RNA polymerase II mediator, can decrease the expression of genes involved in glycolysis and increase the expression of genes involved in protein synthesis. These mutations may be able to release more ATP for the synthesis of 3-HP[75], yet did not increase the production of 3-HP in strain QLW53 any further (Fig. 5b). The glucose repression on the respiratory pathway may still be too strong that glycolysis and respiration may not be well balanced for

high 3-HP production. We next turned to our recently identified Oca5 that degrade 5-diphosphoinositol 1,2,3,4,6-pentakisphosphate (5-InsP$_7$)[74], which serves as an “energy sensor” to sense ATP concentrations and balances gene expressions in glycolysis and respiration. Indeed, *OCA5* deletion significantly increased 3-HP production from 9.12 g/L in QLW53 to 10.15 g/L in QLW58 (Fig. 5b). To verify it is because of the rebalance of glycolysis and respiration rather than simply enhanced respiration, we tested the cultivation in baffled shake flask that could provide more oxygen for oxidative phosphorylation, and indeed the 3-HP production did not improve for QLW53 (Fig. 5b). We also tested the deletion of *OCA3*[76] and upregulation of *KCS1*[77], respectively, that could also increase 5-InsP$_7$ concentrations, yet they did not further improve 3-HP production in QLW58.

The Dual Nature of Uga1: A Double-Edged Sword for 3-HP Production

The structural similarity between 3-HP and serine allowed us to identify the serine dehydrogenase Ora1 for 3-HP production (Fig. 2d), while the isomerized relation of lactate with 3-HP allowed us to identify the first 3-HP permease Esbp6 in yeast (Fig. 3b). Thus, we hypothesized that these similarities may also allow native enzymes to mediate the degradation of 3-HP or its intermediates (Fig. 6a). We started by deleting lactate dehydrogenases Dld1, Dld2, and Dld3, respectively, yet none of the deletions increased 3-HP production (Fig. 6b).

Moreover, it was demonstrated that the gamma-aminobutyrate (GABA) transaminase Uga1 exhibited substrate promiscuity and could convert *β*-alanine to MSA for 3-HP production[78], while studies have also used Uga1 to convert MSA to *β*-alanine in the *β*-alanine auxotroph *E. coli*[19]. These reports indicated that the Uga1 catalysed reaction is reversible, and it may also degrade MSA back to pyruvate, leading to energy waste and decreasing the yield of 3-HP (Fig. 6a). We therefore deleted *UGA1* in the strain and observed a slight increase in 3-HP production to 10.37 g/L in QLW65 (Fig. 6b). We also deleted alanine transaminases Alt1 and Alt2 that convert pyruvate to alanine, respectively, but this had no impact on the production of 3-HP (Fig. 6b). The deletion of *UGA2* to prevent the potential degradation of MSA to malonate did not improve the production of 3-HP, either (Fig. 6b). We believe that the *UGA1* deletion only slightly increased 3-HP production because the generation of MSA was restricted. Therefore, we used the strong promoters *CCW12* and *TDH3* to express the MCR-C domain protein (Fig. 6b). The strain with a strong *CCW12* promoter could increase 3-HP production to 10.77 g/L, indicating that MSA production had improved. We further deleted *UGA1* in this QLW69 strain and indeed increased 3-HP production to 11.25 g/L (Fig. 6b). To our knowledge, this is the first report demonstrating the potential degradation of 3-HP intermediate MSA by the native enzyme in yeast. Our results also underscored the importance that when introducing exogenous metabolite production, the substrate promiscuity bidirectional crosstalk between the target product and the native metabolic network needs to be taken into consideration.

Production of 3-HP by the engineered strain enabled efficient conversion to acrylate

By implementing carbon conservation and energy metabolism strategies, we were able to continuously enhance the carbon yield of both 3-HP and biomass, exceeding yeast limit for 3-HP production in terms of bicarbonate accessible under both respiration and fermentation conditions, close to the theoretical yield with concurrent biomass formation (Fig. 1a and Fig. 7a). Meanwhile, the production envelope analysis also revealed a carbon flux competition between the 3-HP production and biomass generation. With the superposition of multiple strategies, the available carbon resources were insufficient to simultaneously accumulate high levels of both 3-HP and biomass. For example, further rewiring the carbon flux to 3-HP from QLW58 to QLW71, the strain could only move to the top left along the production envelope curve and result in less biomass (Fig. 7a). Importantly, the yield of QLW71 had reached the production envelope boundary of the bicarbonate supplementation equal to the glucose supplementation.

Through this significant rewiring of carbon flux, we achieved the highest 3-HP yield reported. This significantly facilitated the downstream processing, that after simple centrifugation to remove cell pellets, the medium could be directly utilized for acrylate generation. Indeed, the 3-HP present in the medium underwent facile dehydration, facilitated by TiO_2 as a catalyst, ultimately yielding acrylate with a remarkable transformation ratio of 100% (Fig. 7b).

Conclusion

Here we employed the production envelope analysis to demonstrate the crucial role of a high flux of bicarbonate in the production of the platform chemical 3-HP. We identified that the limited availability of bicarbonate has been a major obstacle in previous attempts to produce 3-HP (Fig. 1b), while our strategies of thorough analysis and rewiring of the native bicarbonate metabolism combined with external bicarbonate supply, enabled us to surpass this bicarbonate limitation for 3-HP production. Furthermore, to meet the energy demand for bicarbonate utilization, we employed the 5-InsP_7 mechanism to enhance the ATP generation yield. Additionally, we implemented measures to reduce energy consumption, such as identifying an exporter for 3-HP to minimize energy waste during the 3-HP fermentation process. Moreover, we disrupted the intermediate metabolites MSA degradation pathway to prevent the occurrence of energy futile cycles. Collectively, we were able to achieve the in-flux of bicarbonate for 3-HP equivalent to that of glucose. Ultimately, in the QLW71 strain, the yield of 3-HP to substrate reached an impressive 0.5625 g/g, which corresponds to 89.3% of the theoretical yield with biomass generation. This achievement surpassed the production envelope boundary of bicarbonate (Fig. 7a).

The pursuit of a circular and sustainable carbon economy is a key driver for development of biofuel and biobased chemical production from sustainable carbon sources. However, the net impact of biofuel use on global CO_2 emissions is still under debate[79, 80], leading to continued iterative development[81]. Carbon negativity strategies, such as capturing CO_2 or one-carbon feedstock into biomass or target molecules directly, have been proposed but require large energy inputs and may still result in CO_2 emissions[82–84]. Our research focused on the high carbon yield production of 3-HP using a multi-strategy approach.

Biobased commodity bulk chemicals require high feedstock and carbon yields to achieve economic efficacy and compete with petrochemical-based industries[85]. The pathway for the production of these bulk chemicals must also decrease CO_2 release during glucose oxidation to have commercial potential. Our research provides a step towards the development of sustainable and circular carbon economies for biofuel and biobased chemical production.

Declarations

Acknowledgements

This work was supported by National Key Research and Development Program of China (2018YFA0900100), National Natural Science Foundation of China (22078012), Fundamental Research Funds for the Central Universities (buctrc202304), the Beijing Advanced Innovation Centre for Soft Matter Science and Engineering, Beijing University of Chemical Technology, the Novo Nordisk Foundation (NNF10CC1016517) and the Swedish Research Council FORMAS. This paper was edited using ChatGPT. We also thank Professor Jiqin Zhu from Beijing University of Chemical Technology for his kind help on the acrylic acid experiment.

Author contributions

N.Q., Z.L., Yun C., and J.N. designed the research; N.Q., L.L., X.W., X.J., Yu C., C.L., P.L., Y.Z., W.Y., and J.J. carried out the experiment; N.Q., L.L., J.X., S.S., T.T., J.N., Yun C., and Z.L. analysed the data; N.Q., J.N., Yun. C., and Z.L. wrote the paper; J.N., Yun C., and Z.L. supervised the research. N.Q. and L.L. contributed equally.

Declaration of interests

The authors declare no competing interests.

Methods

Strains, chemicals, and genetic manipulation

An *S. cerevisiae* strain CEN.PK 113-11C (*MATa SUC2 MAL2-8^c his3Δ1 ura3-52*)[54] was used as the experimental model in this study. All the derivatives strains and their genotypes used in this study were listed in Table S2. For the production of 3-HP, the defined minimal medium[55] was used. In detail, the medium consisted of 7.5 g/L $(NH_4)_2SO_4$, 14.4 g/L KH_2PO_4, and 0.5 g/L $MgSO_4{\cdot}7H_2O$ (the pH of the medium was adjusted to 6.5 with KOH). Trace metal and vitamin solutions were supplemented after the medium was autoclaved at 121 °C for 20 min. Histidine (60 mg/L) and uracil (60 mg/L) were

supplemented based on the auxotroph of the plasmid. The calcium carbonate and the sodium bicarbonate were added if needed. To test the dry cell weight (DCW) after the fermentation, the 14.4 g/L KH_2PO_4 in the medium with the calcium carbonate fermentation was changed to 3.0 g/L KH_2PO_4 same as the medium reported for bioreactor cultivations[86]. For the medium with MES buffer, 100mM MES monohydrate was added to the defined minimal medium till the pH was adjusted to 6.5. The carbon source in all the media was 20 g/L glucose. The 3-HP standard was purchased from TCI (TCI, H0297). $NaH^{13}CO_3$ was purchased from Sigma-Aldrich (Sigma-Aldrich, 372382), 2-(*N*-morpholino) ethanesulfonic acid (MES) monohydrate was purchased from Sigma-Aldrich (Sigma-Aldrich, 69892), Nile red was purchased from (ThermoFisher, N1142). Other chemicals including analytical standards were purchased from Sinopharm Chemical (Beijing, China). All genome modifications were carried out using the GTR-CRISPR system[56]. All plasmids were constructed by Golden Gate assembly. The MCR used in this study was from *Chloroflexus aurantiacus*[20], phosphoketolase with substrate specificity to xylulose-5-phosphate was from *Leuconostoc mesenteroides*[20], and phosphotransacetylase was from *Clostridium kluyveri*[21]. The gene of serine dehydrogenase Ora1 was amplified from the genome of the WT *S. cerevisiae* strain. The $NADP^+$-dependent dehydrogenase ydfG was amplified from the genome of *E. coli* MG 1655. All genes were codon-optimized to *S. cerevisiae* and synthesized by Sangon Biotech (Shanghai, China) if not specified. Details of strains, and DNA fragments were summarized in Tables S2 and S3, respectively.

Growth analysis and shake flask fermentation

The strain used for 3-HP production was precultured in the defined minimal medium, then inoculated into a 100 mL shake flask containing 20 mL of the defined minimal medium with a final optical density at 600 nm (OD_{600}) of 0.1. The shake-flask fermentation was carried out at 30 ℃ and 220 rpm for 72 h for 3-HP production. The samples' DCW was measured as reported[74]. The biomass composition of $CH_{1.8}O_{0.5}N_{0.2}$ was assumed[61].

Analytical methods

Concentrations of 3-HP, glucose, and extracellular metabolites were determined using high-performance liquid chromatography (HPLC, Shimadzu, Japan) with an Aminex HPX-87H column (Bio-Rad, Hercules, USA) at 65 ℃, using 0.5 mM H_2SO_4 as the mobile phase at 0.4 mL/min flow rate for 36 min[17].

Gene expression analysis by quantitative real-time PCR (qRT-PCR)

Samples for qRT-PCR analysis were taken when the OD_{600} of the cells reached around 1. The cell pellet was collected by centrifugation at -20 °C, quenched by liquid nitrogen, and stored at -80 °C before use. The RNeasy Mini Kit (QIAGEN, USA) was used for the extraction of total RNA as recommended. The QuantiTect Reverse Transcription Kit (QIAGEN, USA) was used for reverse transcription. 2 µL of produced cDNA was used as the template of the qPCR reaction with the DyNAmo Flash SYBR Green qPCR Kit (Thermo Scientific, USA). Quantitative RT-PCR was performed on Stratagene Mx3005P (Agilent

Technologies, USA). The housekeeping gene *ACT1* was selected as the reference gene. All the primers were listed in Table S3.

Catalytic dehydration of 3-HP to acrylic acid

Acrylic acid synthesis was carried out in a fixed-bed tubular reactor (i.d. = 8 mm, o.d. = 12 mm, length = 30 cm) according the method mentioned in the previous research[14]. After culturing the strains for 72 hours in a defined minimal medium, the fermentation broth was sterilized by filtration and diluted 6 times with ultrapure water. And then 3 g TiO_2 as the catalyst (20-40 mesh) was loaded into the reactor tube between two layers of quartz wool and preheated at 230 ℃ in the furnace. The diluted fermentation broth was delivered using a metering pump with a rate of 100 mL/h for 5 minutes, and then with a constant rate of 1.5 mL/h. The eluate containing acrylic acid was condensed in a cold-water bath. Liquid samples of the first 30 min were discarded. Additionally, 4 samples were collected for each measurement.

Genome-scale metabolic modelling

The genome-scale metabolic model of *S. cerevisiae* Yeast8[17], was expanded by adding two heterologous reactions, i.e., malonyl-CoA reduction and MSA reduction, as well as the secretion of 3-HP. The resulting model with the default constraints was used to estimate the yield of 3-HP on glucose. To do so, the uptake rate of glucose was fixed at 1 mmol/gDCW/h, the growth rate was adjusted, and the secretion of 3-HP was maximized for each growth rate. To simulate the effect of native bicarbonate production on the yield, the upper bound on the rate of the bicarbonate formation in the model, which converts carbon dioxide to bicarbonate, was set at different values normalized to the glucose uptake rate. Model simulations were performed using the COBRA toolbox[87] in MATLAB with the CPLEX as an optimization solver.

Phylogenetic analysis

Amino acid sequences from the SLC4 family (InterPro ID: IPR003020) and SLC26 family (InterPro ID: IPR001902) were aligned and trimmed using NGPhylogeny.fr[88]. Only key species (*S. cerevisiae*, *Arabidopsis thaliana,* and *Homo sapiens* for SLC4 and *S. cerevisiae*, *E. coli*, *A. thaliana*, and *H. sapiens* for SLC26) were included. MEGA 11 was used to construct a maximum likelihood phylogenetic tree and tested with 500 bootstraps[89]. iTOL v6 was used in the modification of the phylogenetic tree[90].

Isotope ^{13}C labelling analysis

The minimal medium with 10 mM $NaH^{13}CO_3$ (Sigma-Aldrich) in a shake flask was used for the isotope labelling experiment. Strains were inoculated with OD_{600} 0.01 and sampled after 72 h. For quenching, the method was followed as previously described with some modifications[74]. 2 mL medium was transferred immediately into the 15 mL tube with 8 mL pure methanol (precooling in -80 ℃ fridge) and vortexed around 1s. Then, the mix was centrifuged at 6,000 rpm for 3 min at 4 ℃. Remove the supernatant and resuspend the precipitate with 3 mL of precooling methanol, 6,000 rpm centrifuged for 3 minutes, remove

the supernatant, keep on ice. For hydrolysis of cellular components method was followed as previously described[91] 6 mL 6N hydrochloric acid was added to quenched cells and transferred to 10 mL glass digestion tube, cells were hydrolysed for 16–20 h in metal bath at 115 °C and dried in a heating block at 85 °C, then add 600 µL of ultrapure water, centrifuged at the maximum speed for 1 min. Before the MS analysis, the sample was filtrated with a 0.22 µm pore size filter membrane. The isotopic labels of metabolites were determined with UPLC-MS/MS (SCIEX TRIPLETOF 6600) as previously research[74].

Microscopy imaging

The method of fluorescence microscopy images was as the previously published[92]. After cultured for 72h in the defined minimal medium, 250 µL sample of each yeast cell culture was transferred into a sterile 1.5 mL tube. Then 25 µL freshly prepared DMSO: PBS buffer (1:1) and 5 µg/mL Nile red in acetone (25 µL of freshly prepared 60 µg/mL stock) was added to each sample followed by mixing. The sample was then incubated in the dark for 5 min at room temperature, and washed twice with PBS buffer. 5 µL of the cell sample was pipetted onto a glass microscope slide, placed with the cover slip firmly, and observed using the green fluorescence channel with the excitation wavelength at 488 nm and emission wavelength at 509nm.

Quantification and statistical analysis

All data was presented as mean ± standard deviation (SD) of biological triplicates. Significant comparisons of two groups were indicated in the graphs statistical analysis performed using a two-tailed unpaired Student's t-test (*p < 0.05, **p < 0.01, ***p < 0.001). The graphs represented means ± SD unless otherwise indicated, as described in the figure legends.

References

1. Scown, C.D. & Keasling, J.D. Sustainable manufacturing with synthetic biology. Nat. Biotechnol. 40, 304–307 (2022).
2. Keasling, J. et al. Microbial production of advanced biofuels. Nat. Rev. Microbiol. 19, 701–715 (2021).
3. Liu, Y. et al. Biofuels for a sustainable future. Cell 184, 1636–1647 (2021).
4. Hertel, T.W. et al. Effects of US maize ethanol on global land use and greenhouse gas emissions: estimating market-mediated responses. Bioscience 60, 223–231 (2010).
5. Liu, Z., Wang, K., Chen, Y., Tan, T. & Nielsen, J. Third-generation biorefineries as the means to produce fuels and chemicals from CO_2. Nat. Catal. 3, 274–288 (2020).
6. Baumschabl, M. et al. Conversion of CO_2 into organic acids by engineered autotrophic yeast. *Proc. Natl. Acad. Sci. USA* 119, e2211827119 (2022).
7. Fuchs, G. Alternative pathways of carbon dioxide fixation: insights into the early evolution of life? Annu. Rev. Microbiol. 65, 631–658 (2011).

8. Bianchi, F., Van't Klooster, J.S., Ruiz, S.J. & Poolman, B. Regulation of amino acid transport in *Saccharomyces cerevisiae*. Microbiol. Mol. Biol. Rev. 83, 10–1128 (2019).
9. Berg, I.A. Ecological aspects of the distribution of different autotrophic CO_2 fixation pathways. Appl. *Environ. Microbiol.* 77, 1925–1936 (2011).
10. Berg, I.A., Kockelkorn, D., Buckel, W. & Fuchs, G. A 3-hydroxypropionate/4-hydroxybutyrate autotrophic carbon dioxide assimilation pathway in Archaea. Science 318, 1782–1786 (2007).
11. Zarzycki, J., Brecht, V., Muller, M. & Fuchs, G. Identifying the missing steps of the autotrophic 3-hydroxypropionate CO_2 fixation cycle in *Chloroflexus aurantiacus*. *Proc. Natl. Acad. Sci. USA* 106, 21317–21322 (2009).
12. Werpy, T. & Petersen, G. Top value added chemicals from biomass volume I—Results of screening for potential candidates from sugars and synthesis Gas. No. DOE/GO-102004-1992. *National Renewable Energy Lab. (NREL), Golden, CO (United States)* (2004).
13. Zabed, H.M. et al. Biocatalytic gateway to convert glycerol into 3-hydroxypropionic acid in waste-based biorefineries: Fundamentals, limitations, and potential research strategies. Biotechnol. Adv. 62, 108075 (2023).
14. Dishisha, T., Pyo, S.H. & Hatti-Kaul, R. Bio-based 3-hydroxypropionic- and acrylic acid production from biodiesel glycerol via integrated microbial and chemical catalysis. Microb. Cell Fact. 14, 200 (2015).
15. Bhagwat, S.S. et al. Sustainable production of acrylic Acid via 3-hydroxypropionic acid from lignocellulosic biomass. ACS Sustainable Chem. & Eng. 9, 16659–16669 (2021).
16. Yu, W., Cao, X., Gao, J. & Zhou, Y.J. Overproduction of 3-hydroxypropionate in a super yeast chassis. Bioresour. Technol. 361, 127690 (2022).
17. Lu, H. et al. A consensus *S. cerevisiae* metabolic model Yeast8 and its ecosystem for comprehensively probing cellular metabolism. Nat. Commun. 10, 3589 (2019).
18. Canelas, A.B. et al. Integrated multilaboratory systems biology reveals differences in protein metabolism between two reference yeast strains. Nat. Commun. 1, 145 (2010).
19. Liu, C. et al. Functional balance between enzymes in malonyl-CoA pathway for 3-hydroxypropionate biosynthesis. Metab. Eng. 34, 104–111 (2016).
20. Qin, N. et al. Rewiring central carbon metabolism ensures increased provision of acetyl-CoA and NADPH required for 3-OH-propionic acid production. *ACS Synth. Biol.* 9, 3236–3244 (2020).
21. Chen, X., Yang, X., Shen, Y., Hou, J. & Bao, X. Increasing malonyl-CoA derived product through controlling the transcription regulators of phospholipid synthesis in *Saccharomyces cerevisiae*. *ACS Synth. Biol.* 6, 905–912 (2017).
22. Ouyang, L., Holland, P., Lu, H., Bergenholm, D. & Nielsen, J. Integrated analysis of the yeast NADPH-regulator Stb5 reveals distinct differences in NADPH requirements and regulation in different states of yeast metabolism. FEMS Yeast Res. 18, foy091 (2018).
23. Christodoulou, D. et al. Reserve flux capacity in the pentose phosphate pathway enables *Escherichia coli*'s rapid response to oxidative stress. *Cell Syst.* 6, 569–578.e567 (2018).

24. Kim, J.E., Jang, I.S., Sung, B.H., Kim, S.C. & Lee, J.Y. Rerouting of NADPH synthetic pathways for increased protopanaxadiol production in *Saccharomyces cerevisiae*. Sci. Rep. 8, 15820 (2018).
25. Curran, K.A. et al. Design of synthetic yeast promoters via tuning of nucleosome architecture. Nat. Commun. 5, 4002 (2014).
26. Xiao, M., Zhu, X., Bi, C., Ma, Y. & Zhang, X. Improving succinate productivity by engineering a cyanobacterial CO_2 concentrating system (CCM) in *Escherichia coli.* Biotechnol. J. 12, 1700199 (2017).
27. Yu, J.H. et al. Combinatorial optimization of CO_2 transport and fixation to improve succinate production by promoter engineering. Biotechnol. Bioeng. 113, 1531–1541 (2016).
28. Aguilera, J., Van Dijken, J.P., De Winde, J.H. & Pronk, J.T. Carbonic anhydrase (Nce103p): an essential biosynthetic enzyme for growth of *Saccharomyces cerevisiae* at atmospheric carbon dioxide pressure. Biochem. J. 391, 311–316 (2005).
29. Cordat, E. & Reithmeier, R.A. Structure, function, and trafficking of SLC4 and SLC26 anion transporters. Curr. Top Membr. 73, 1–67 (2014).
30. Jennings, M.L., Howren, T.R., Cui, J., Winters, M. & Hannigan, R. Transport and regulatory characteristics of the yeast bicarbonate transporter homolog Bor1p. Am. J. Physiol. Cell Physiol. 293, C468-476 (2007).
31. Alper, S.L. & Sharma, A.K. The SLC26 gene family of anion transporters and channels. Mol. Aspects Med. 34, 494–515 (2013).
32. Leves, F.P., Tierney, M.L. & Howitt, S.M. Polar residues in a conserved motif spanning helices 1 and 2 are functionally important in the SulP transporter family. Int. J. Biochem. Cell Biol. 40, 2596–2605 (2008).
33. Guo, X. et al. Ptc7p Dephosphorylates select mitochondrial proteins to enhance metabolic function. Cell Rep. 18, 307–313 (2017).
34. Guo, X., Niemi, N.M., Coon, J.J. & Pagliarini, D.J. Integrative proteomics and biochemical analyses define Ptc6p as the *Saccharomyces cerevisiae* pyruvate dehydrogenase phosphatase. *J.* Biol. Chem. 292, 11751–11759 (2017).
35. Yu, T. et al. Reprogramming Yeast metabolism from alcoholic fermentation to lipogenesis. Cell 174, 1549–1558 (2018).
36. Usaite, R. et al. Reconstruction of the yeast Snf1 kinase regulatory network reveals its role as a global energy regulator. Mol. Syst. Biol. 5, 319 (2009).
37. Wang, S. et al. The expression modulation of the key enzyme Acc for highly efficient 3-hydroxypropionic acid production. Front. Microbiol. 13, 902848 (2022).
38. Shi, S., Chen, Y., Siewers, V. & Nielsen, J. Improving production of malonyl coenzyme A-derived metabolites by abolishing Snf1-dependent regulation of Acc1. *MBio.* 5, e01130-01114 (2014).
39. Son, H.F. et al. Structural insight into bi-functional malonyl-CoA reductase. Environ. Microbiol. 22, 752–765 (2020).

40. Zhu, Z. et al. Expanding the product portfolio of fungal type I fatty acid synthases. Nat. Chem. Biol. 13, 360–362 (2017).
41. Tong, T. et al. A biosynthesis pathway for 3-hydroxypropionic acid production in genetically engineered *Saccharomyces cerevisiae*. Green Chem. 23, 4502–4509 (2021).
42. Qin, N., Li, L., Wang, Z. & Shi, S. Microbial production of odd-chain fatty acids. Biotechnol. Bioeng. 120, 917–931 (2022).
43. Keren, L. et al. Promoters maintain their relative activity levels under different growth conditions. Mol. Syst. Biol. 9, 701 (2013).
44. Peetermans, A., Foulquie-Moreno, M.R. & Thevelein, J.M. Mechanisms underlying lactic acid tolerance and its influence on lactic acid production in *Saccharomyces cerevisiae*. Microb. Cell 8, 111–130 (2021).
45. Kildegaard, K.R. et al. Evolution reveals a glutathione-dependent mechanism of 3-hydroxypropionic acid tolerance. Metab. Eng. 26, 57–66 (2014).
46. Xu, X., Williams, T.C., Divne, C., Pretorius, I.S. & Paulsen, I.T. Evolutionary engineering in *Saccharomyces cerevisiae* reveals a *TRK1*-dependent potassium influx mechanism for propionic acid tolerance. Biotechnol. Biofuels. 12, 97 (2019).
47. Chun, A.Y., Yunxiao, L., Ashok, S., Seol, E. & Park, S. Elucidation of toxicity of organic acids inhibiting growth of *Escherichia coli* W. Biotech. and Biopro. Eng. 19, 858–865 (2014).
48. van Maris, A.J., Konings, W.N., van Dijken, J.P. & Pronk, J.T. Microbial export of lactic and 3-hydroxypropanoic acid: implications for industrial fermentation processes. Metab. Eng. 6, 245–255 (2004).
49. Lee, J.J., Crook, N., Sun, J. & Alper, H.S. Improvement of lactic acid production in *Saccharomyces cerevisiae* by a deletion of *ssb1*. J. *Ind. Microbiol. Biotechnol.* 43, 87–96 (2016).
50. Sherwood, P.W. & Carlson, M. Efficient export of the glucose transporter Hxt1p from the endoplasmic reticulum requires Gsf2p. *Proc. Natl. Acad. Sci. USA* 96, 7415–7420 (1999).
51. Darbani, B., Stovicek, V., van der Hoek, S.A. & Borodina, I. Engineering energetically efficient transport of dicarboxylic acids in yeast *Saccharomyces cerevisiae. Proc. Natl. Acad. Sci. USA* 116, 19415–19420 (2019).
52. Baek, S.H. et al. Improvement of D-lactic acid production in *Saccharomyces cerevisiae* under acidic conditions by evolutionary and rational metabolic engineering. Biotechnol. J. 12, 1700015 (2017).
53. Dato, L. et al. Changes in *SAM2* expression affect lactic acid tolerance and lactic acid production in *Saccharomyces cerevisiae*. Microb. Cell Fact. 13, 147 (2014).
54. Nygard, Y. et al. The diverse role of Pdr12 in resistance to weak organic acids. Yeast 31, 219–232 (2014).
55. Viegas, C.A., Sebastiao, P.B., Nunes, A.G. & Sa-Correia, I. Activation of plasma membrane H(+)-ATPase and expression of *PMA1* and *PMA2* genes in *Saccharomyces cerevisiae* cells grown at supraoptimal temperatures. Appl. Environ. Microbiol. 61, 1904–1909 (1995).

56. Orij, R., Brul, S. & Smits, G.J. Intracellular pH is a tightly controlled signal in yeast. Biochim. Biophys. Acta 1810, 933–944 (2011).
57. Sugiyama, M., Akase, S.P., Nakanishi, R., Kaneko, Y. & Harashima, S. Overexpression of *ESBP6* improves lactic acid resistance and production in *Saccharomyces cerevisiae*. J. Biosci. Bioeng. 122, 415–420 (2016).
58. Casal, M., Paiva, S., Andrade, R.P., Gancedo, C. & Leão, C.I. The lactate-proton symport of *Saccharomyces cerevisiae* is encoded by *JEN1*. J. Bacteriol. 181, 2620–2623 (1999).
59. Pacheco, A. et al. Lactic acid production in *Saccharomyces cerevisiae* is modulated by expression of the monocarboxylate transporters Jen1 and Ady2. FEMS Yeast Res. 12, 375–381 (2012).
60. Baek, S.H., Kwon, E.Y., Kim, S.Y. & Hahn, J.S. *GSF2* deletion increases lactic acid production by alleviating glucose repression in *Saccharomyces cerevisiae*. Sci. Rep. 6, 34812 (2016).
61. Baek, S.H., Kwon, E.Y., Kim, Y.H. & Hahn, J.S. Metabolic engineering and adaptive evolution for efficient production of D-lactic acid in *Saccharomyces cerevisiae*. Appl. Microbiol. Biotechnol. 100, 2737–2748 (2016).
62. Serre, V. et al. Half of *Saccharomyces cerevisiae* carbamoyl phosphate synthetase produces and channels carbamoyl phosphate to the fused aspartate transcarbamoylase domain. J. Biol. Chem. 274, 23794–23801 (1999).
63. Ali, E.S. et al. The mTORC1-SLC4A7 axis stimulates bicarbonate import to enhance *de novo* nucleotide synthesis. Mol. Cell 82, 3284–3298.e7 (2022).
64. Winkler, M.E. & Ramos-Montanez, S. Biosynthesis of Histidine. *EcoSal Plus* 3, 10–1128(2009).
65. Alam, M.T. et al. The metabolic background is a global player in *Saccharomyces* gene expression epistasis. Nat. Microbiol. 1, 15030 (2016).
66. Yan, C. et al. Auxotrophs compromise cell growth and fatty acid production in *Saccharomyces cerevisiae*. Biotechnol. J. 18, e2200510 (2023).
67. Yu, R. et al. Nitrogen limitation reveals large reserves in metabolic and translational capacities of yeast. Nat. Commun. 11, 1881 (2020).
68. Malubhoy, Z. et al. Carbon dioxide fixation via production of succinic acid from glycerol in engineered *Saccharomyces cerevisiae*. Microb. Cell Fact. 21, 102 (2022).
69. Lopez-Garzon, C.S. & Straathof, A.J. Recovery of carboxylic acids produced by fermentation. Biotechnol. Adv. 32, 873–904 (2014).
70. Rodriguez, A., De La Cera, T., Herrero, P. & Moreno, F. The hexokinase 2 protein regulates the expression of the *GLK1*, *HXK1* and *HXK2* genes of *Saccharomyces cerevisiae. Biochem. J.* 355, 625–631 (2001).
71. Stoddard, P.R. et al. Polymerization in the actin ATPase clan regulates hexokinase activity in yeast. Science 367, 1039–1042 (2020).
72. Bakker, B.M. et al. Stoichiometry and compartmentation of NADH metabolism in *Saccharomyces cerevisiae*. FEMS Microbiol. Rev. 25, 15–37 (2001).

73. Moreno, F. & Herrero, P. The hexokinase 2-dependent glucose signal transduction pathway of *Saccharomyces cerevisiae*. FEMS Microbiol. Rev. 26, 83–90 (2002).
74. Qin, N. et al. Flux regulation through glycolysis and respiration is balanced by inositol pyrophosphates in yeast. Cell 186, 748–763 (2023).
75. Dai, Z., Huang, M., Chen, Y., Siewers, V. & Nielsen, J. Global rewiring of cellular metabolism renders *Saccharomyces cerevisiae* Crabtree negative. Nat. Commun. 9, 3059 (2018).
76. Steidle, E.A. et al. A novel inositol pyrophosphate phosphatase in *Saccharomyces cerevisiae*. J. Biol. Chem. 291, 6772–6783 (2016).
77. Szijgyarto, Z., Garedew, A., Azevedo, C. & Saiardi, A. Influence of inositol pyrophosphates on cellular energy dynamics. Science 334, 802–805 (2011).
78. Borodina, I. et al. Establishing a synthetic pathway for high-level production of 3-hydroxypropionic acid in *Saccharomyces cerevisiae* via beta-alanine. Metab. Eng. 27, 57–64 (2015).
79. Müller, L.J. et al. A Guideline for life cycle assessment of carbon capture and utilization. Frontiers in Energy Research 8, 15(2020).
80. DeCicco, J.M. et al. Carbon balance effects of U.S. biofuel production and use. Clim. Change 138, 667–680 (2016).
81. Marcellin, E. et al. Low carbon fuels and commodity chemicals from waste gases – systematic approach to understand energy metabolism in a model acetogen. Green Chem. 18, 3020–3028 (2016).
82. Gleizer, S. et al. Conversion of *Escherichia coli* to generate all biomass carbon from CO_2. Cell 179, 1255–1263.e1212 (2019).
83. Chen, F.Y., Jung, H.W., Tsuei, C.Y. & Liao, J.C. Converting *Escherichia coli* to a synthetic methylotroph growing solely on methanol. *Cell* 182, 933–946 e914 (2020).
84. Antonovsky, N. et al. Sugar synthesis from CO_2 in *Escherichia coli*. Cell 166, 115–125 (2016).
85. Hu, G. et al. Light-driven CO_2 sequestration in *Escherichia coli* to achieve theoretical yield of chemicals. *Nat. Catal.* 4, 395–406 (2021).
86. Liu, Q. et al. Rewiring carbon metabolism in yeast for high level production of aromatic chemicals. Nat. Commun. 10, 4976 (2019).
87. Heirendt, L. et al. Creation and analysis of biochemical constraint-based models using the COBRA Toolbox v.3.0. Nat. Protoc. 14, 639–702 (2019).
88. Lemoine, F. et al. NGPhylogeny.fr: new generation phylogenetic services for non-specialists. Nucleic Acids Res. 47, W260-W265 (2019).
89. Tamura, K., Stecher, G. & Kumar, S. MEGA11: Molecular evolutionary genetics analysis version 11. Mol. Biol. Evol. 38, 3022–3027 (2021).
90. Letunic, I. & Bork, P. Interactive Tree Of Life (iTOL) v5: an online tool for phylogenetic tree display and annotation. Nucleic Acids Res. 49, W293-W296 (2021).

91. Canelas, A.B. et al. Quantitative evaluation of intracellular metabolite extraction techniques for yeast metabolomics. Anal. Chem. 81, 7379–7389 (2009).
92. Rostron, K.A. & Lawrence, C.L. Nile red staining of neutral lipids in yeast. *Methods Mol. Biol.* 1560, 219–229 (Springer, 2017).
93. Li, S., Si, T., Wang, M. & Zhao, H. Development of a synthetic malonyl-CoA sensor in *Saccharomyces cerevisiae* for intracellular metabolite monitoring and genetic screening. *ACS Synth. Biol.* 4, 1308–1315 (2015).
94. David, F., Nielsen, J. & Siewers, V. Flux control at the malonyl-CoA node through hierarchical dynamic pathway regulation in *Saccharomyces cerevisiae*. *ACS Synth. Biol*. 5, 224–233 (2016).
95. Zhang, Y., Su, M., Wang, Z., Nielsen, J. & Liu, Z. Rewiring regulation on respiro-fermentative metabolism relieved Crabtree effects in *Saccharomyces cerevisiae*. *Synth. and Sys. Biotech.* (2022).
96. Kildegaard, K.R. et al. Engineering and systems-level analysis of *Saccharomyces cerevisiae* for production of 3-hydroxypropionic acid via malonyl-CoA reductase-dependent pathway. Microb. Cell Fact. 15, 53 (2016).
97. Zhang, Y. et al. Engineering yeast mitochondrial metabolism for 3-hydroxypropionate production. *Biotech. for Biofuels. and Bioprod*. 16, 1–11 (2023).

Figures

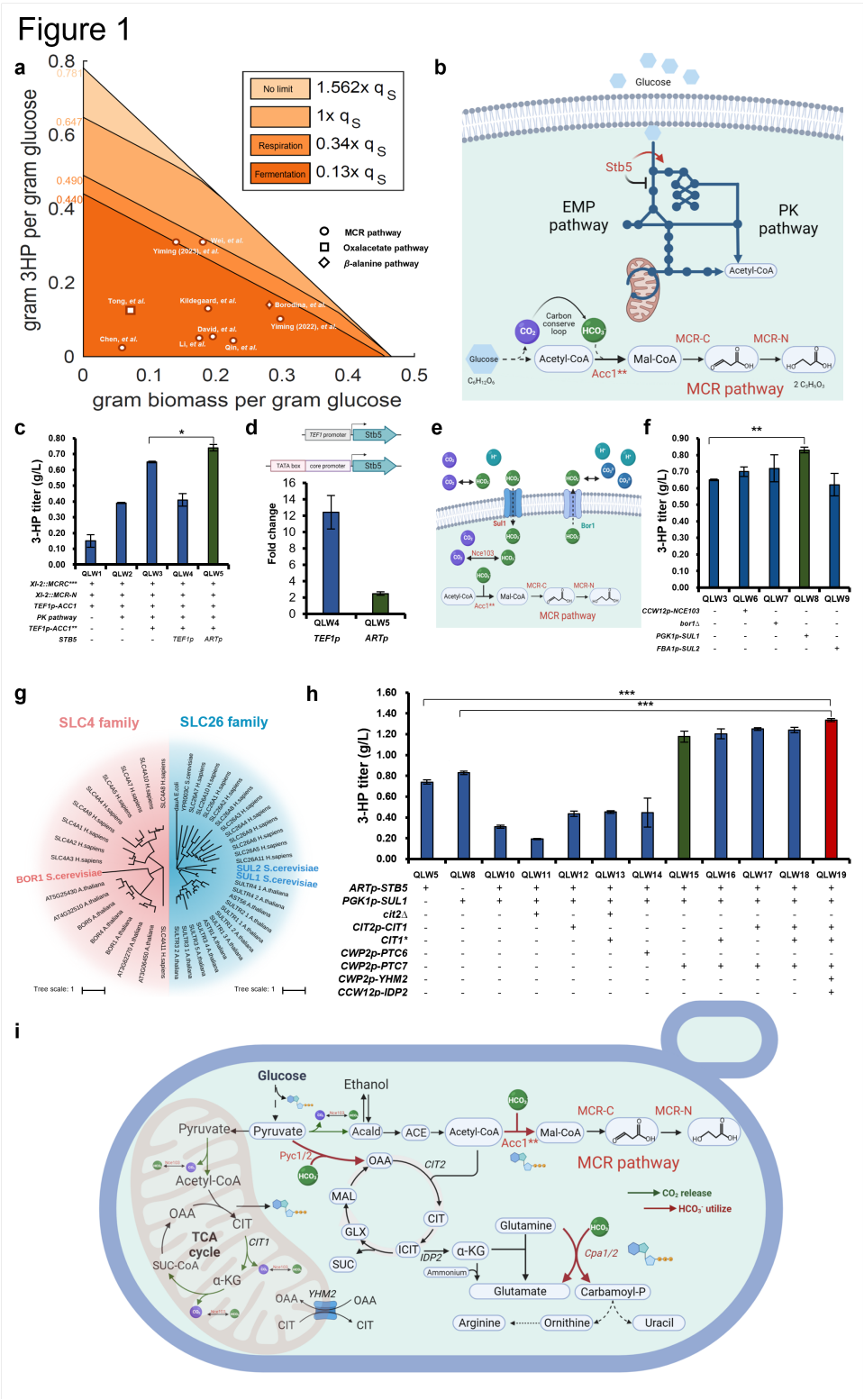

Figure 1

Production envelope analysis and bicarbonate metabolism rewiring for CO_2 fixation. (**a**) The production envelope analysis based on the Yeast8 model with the malonyl-CoA reductase reaction for 3-HP production. Different colour represented the range of 3-HP production with its concurrent biomass under different bicarbonate flux. Here, we assume bicarbonate can be freely converted from CO_2. The X and Y axis indicated biomass yield to glucose (g/g) and 3-HP yield to glucose (g/g), respectively. Reports used

the malonyl-CoA pathway[16, 20, 21, 93-97], the oxaloacetate pathway[41], and the *β* alanine pathway[78] were labelled with dot, square, and diamond, respectively. The q_S indicated the consumed rate of glucose, the flux boundary of bicarbonate of respiration and fermentation was calculated based on the previous research[18]. The DCW was calculated by 0.7* OD_{600} if there was no biomass reported in the research. (**b**) The malonyl-CoA reductase pathway was used to produce 3-HP in this study, that acetyl-CoA and bicarbonate were first transformed to malonyl-CoA by Acc1**, and then to 3-HP by the MCR-C domain and MCR-N domain. Transcription factor Stb5 could realize the carbon flux rewiring from glycolysis to the oxPP pathway, thus increasing the flux through the xPK pathway and reduce the CO_2 release. (**c**) Adjusting *STB5* expression by *ARTp* could together with the expression optimization of MCR domains, Acc1 and the PK pathway enhanced 3-HP production to 0.74 g/L. (**d**) Substitution of the native promoter of Stb5 with the *TEF1p* and an artificial promoter *ARTp*, respectively, and quantification of the *STB5* with *TEF1*p and *ARTp* strength by qPCR. (**e**) Cellular bicarbonate derived from the bicarbonate transporter Sul1 (into the cell), Bor1 (outside the cell), and the endogenous synthesis from CO_2 by native carbonic anhydrase Nce103. (**f**) Providing more bicarbonate by overexpressing *SUL1* enhanced 3-HP production to 0.83 g/L. (**g**) Phylogenetic analysis of SLC4 and SLC 26 families identified Bor1, Sul1, and Sul2 as potential bicarbonate transporters in *S. cerevisiae*. (**h**) Rewiring the carbon flux from oxaloacetate to the high production of 3-HP. Overexpressing the phosphatase Ptc7 could significantly increase the 3-HP production based on overexpressing *CIT1*, introducing $Cit1^{S462A}$ mutation, overexpressing the transporter Yhm2 to transport the oxaloacetate into mitochondria, and overexpressing cytosolic NADP-specific isocitrate dehydrogenase Idp2. (**i**) Distribution of CO_2 releasing reaction and bicarbonate utilizing reaction in *S. cerevisiae.* Abbreviations were defined in Table S1. All data were presented as mean ± SD of biological triplicates.

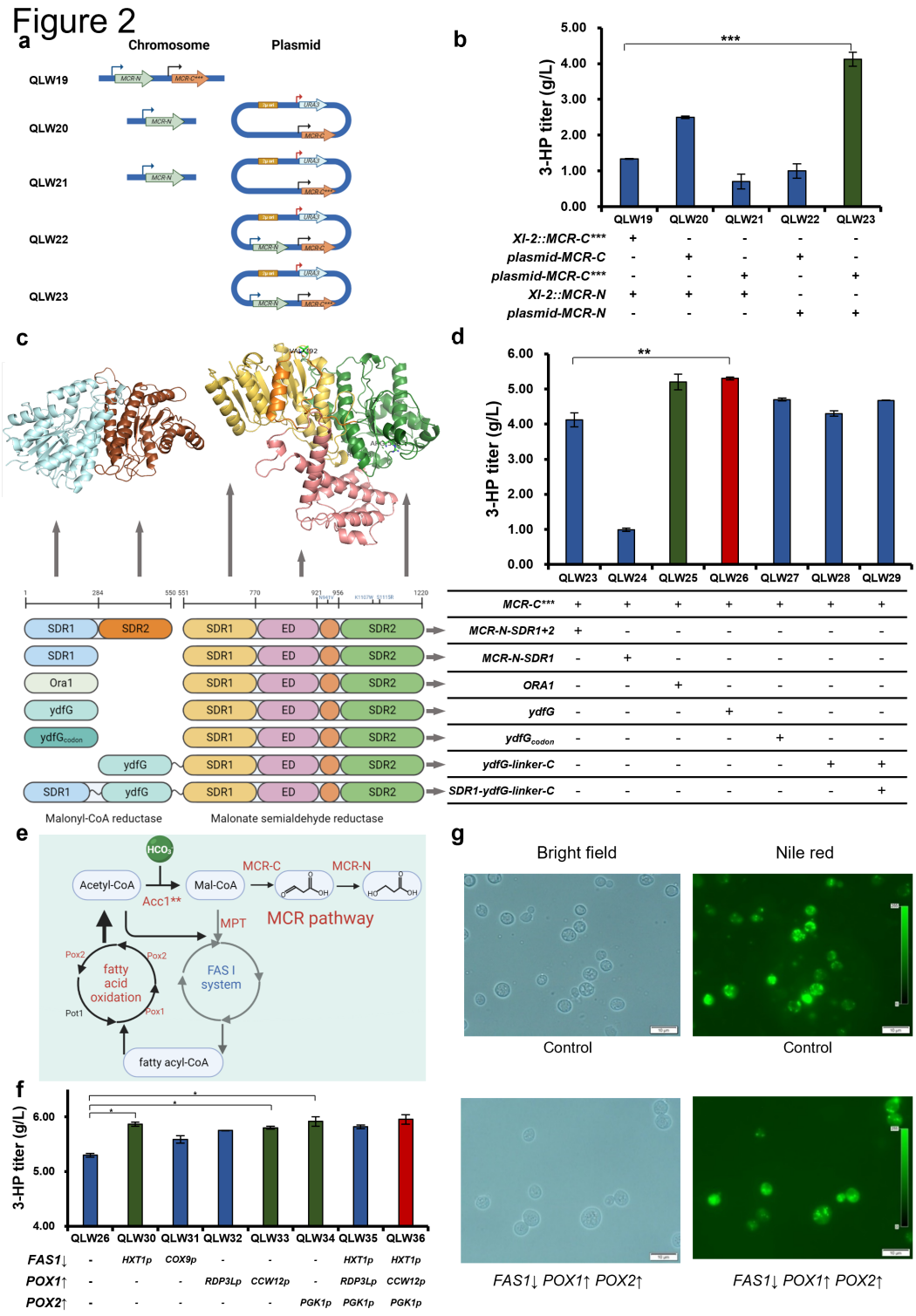

Figure 2

Enzyme and pathway engineering for efficient production of 3-HP.(**a**) Split MCR enzymes were adjusted by their expressions through by chromosome integration and plasmid expression. (**b**) MCR-N domain and MCR-C*** domain were co-expressed with the high copy plasmid could produce 4.12 g/L 3-HP. (**c**) Homologous modelling structure of the domains in malonyl-CoA reductase and malonate semialdehyde reductase from *C. aurantiacus*. (**d**) Swapping of native MCR domains with Ora1 and ydfG improved 3-HP

production to 5.2 g/L and 5.3 g/L, respectively. (**e**) Carbon flux rewiring from fatty acids to 3-HP. (**f**) Downregulation of *FAS1*combined with upregulation of *POX2* and *POX1* improved the production of 3-HP. (**g**) Nile red staining demonstrated that the size and the number of lipid droplets decreased in the fatty acid oxidation strain. Abbreviations were defined in Table S1. All data were presented as mean ± SD of biological triplicates.

Figure 3

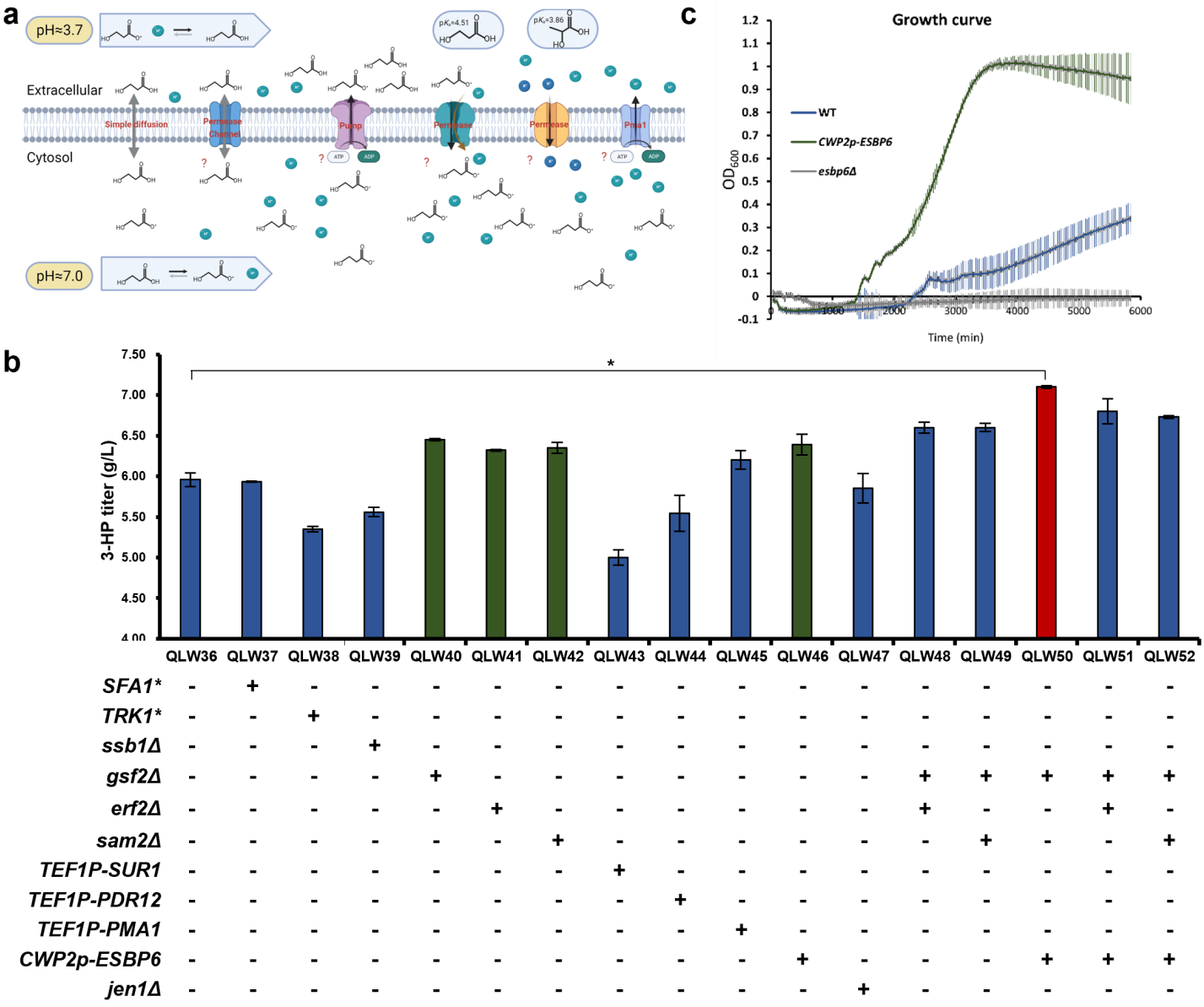

Figure 3

Genotype identification of 3-HP tolerance and increase the production of 3-HP. (**a**) Schematic representation of transporters and permeases in the cell membrane. (**b**) Overexpression of *ESBP6*, deletion of *SAM2*, *GSF2*, or *ERF2* could significantly improve the production of 3-HP. (**c**) Growth profiling

showed that overexpression of *ESBP6* could remarkably increase cell tolerance compared with WT in high concentrations of 3-HP. Abbreviations were defined in Table S1. All data were presented as mean ± SD of biological triplicates.

Figure 4

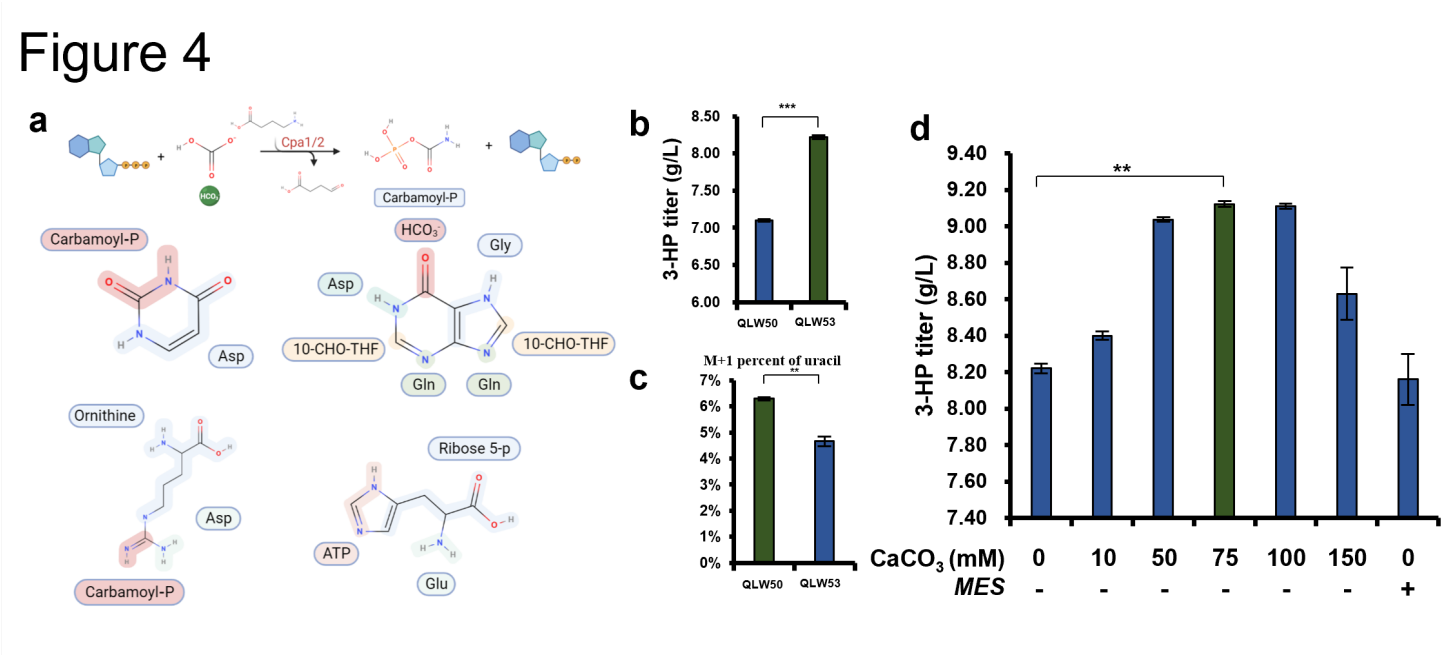

Figure 4

Alleviating bicarbonate competitions from the *de novo* pyridine ring synthesis enhanced 3-HP production. (**a**) Carbamoyl-P was synthesized by Cpa1/2 from ATP, bicarbonate, and glutamate. Atom sources for purine, pyrimidine, arginine, and histidine were marked. (**b**) Substitution of *URA3* marker by *HIS3* marker in the same plasmid background increased the 3-HP titer to 8.22 g/L in the QLW53 strain. (**c**) ^{13}C isotope labelling indicated that less M+1 uracil was produced in QLW53 strain corresponding to the higher 3-HP titer. (**d**) $CaCO_3$ was used to provide more bicarbonate recycling CO_2. Abbreviations were defined in Table S1. All data were presented as mean ± SD of biological triplicates.

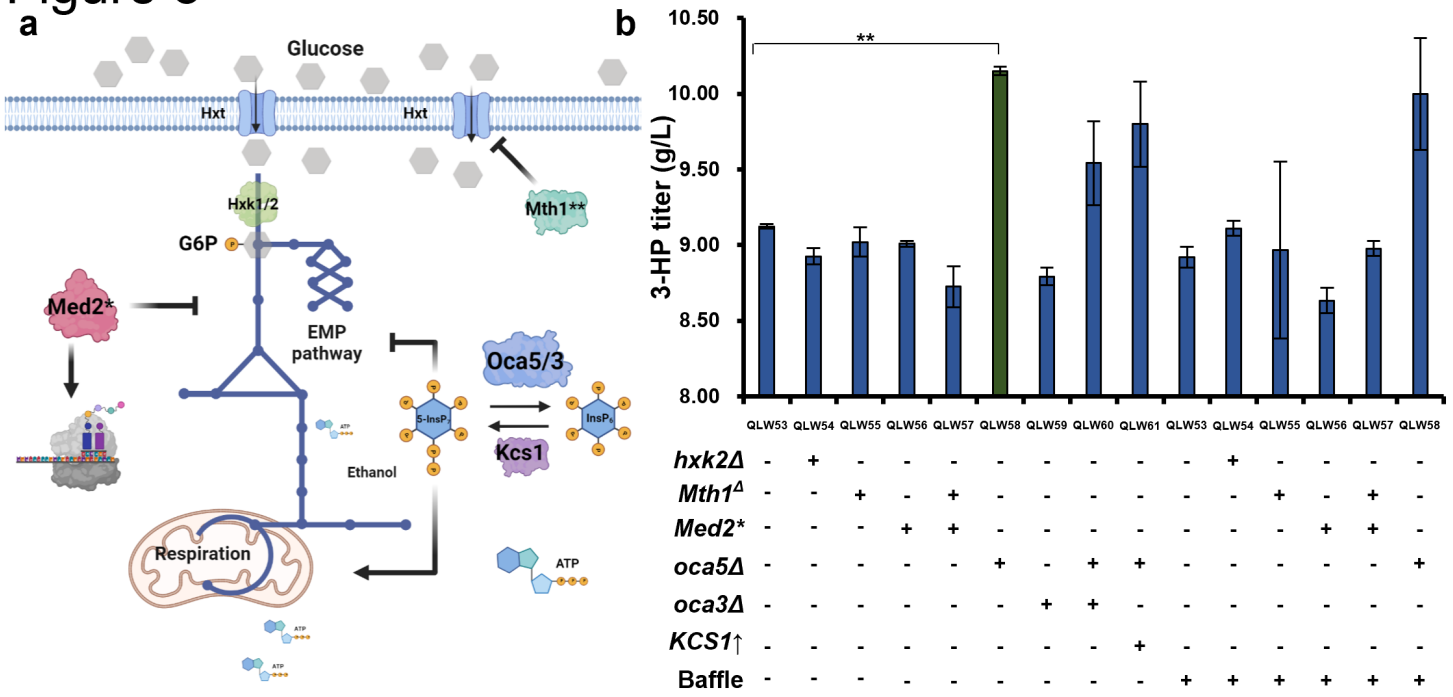

Figure 5

Utilization of inositol pyrophosphate signalling to provide more ATP for 3-HP production. (**a**) Schematic representation of regulation mechanisms involved in glycolysis and respiration in yeast. (**b**) *OCA5*deletion improved the production of 3-HP to 10.15 g/L. Abbreviations were defined in Table S1. All data were presented as mean ± SD of biological triplicates.

Figure 6

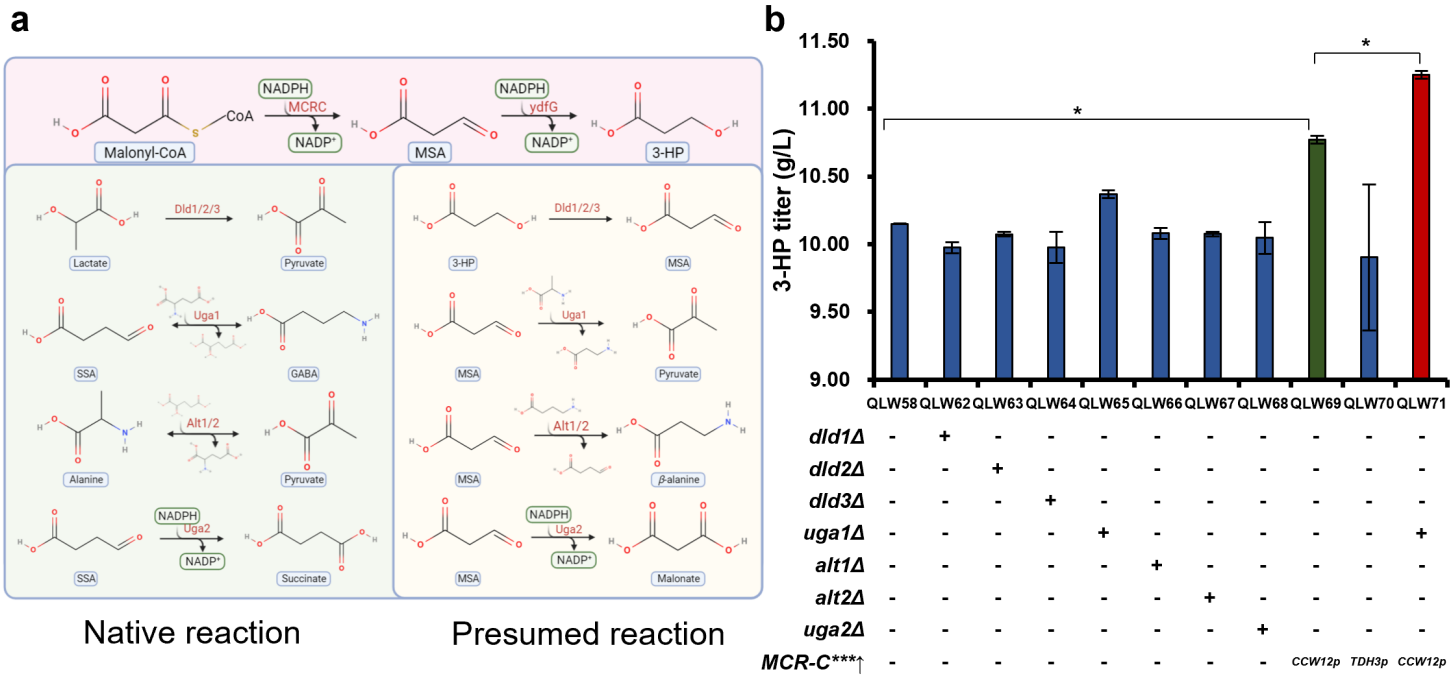

Figure 6

Abolishing potential degradations of MSA improved 3HP production. (**a**) Candidate enzymes that might be able to degrade 3-HP based on the isomerized relation between lactate and 3-HP. (**b**) Deletion of *UGA1* combined with overexpression of the MCR-C domain using *CCW12* promoter could improve the 3-HP production to 11.25 g/L. Abbreviations were defined in Table S1. All data were presented as mean ± SD of biological triplicates.

Figure 7

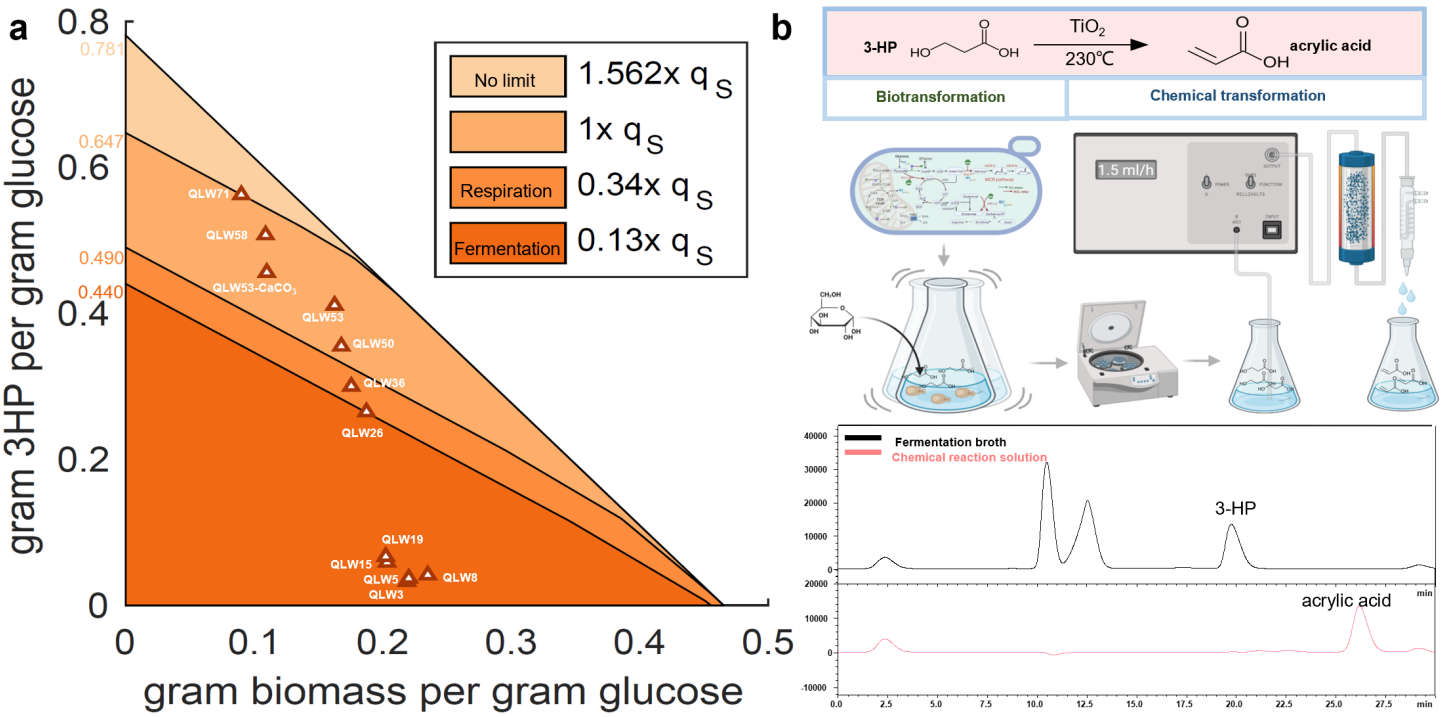

Figure 7

The 3-HP production break the bicarbonate restrict and the medium could directly dehydration to acrylic acid. (**a**) The production envelope incorporated with key 3-HP production results reported in this study. Collectively, four of our constructed strains exceeded the 3-HP production boundary with native metabolisms, with QLW71 approaching the inaccessible one to one ratio of bicarbonate influx versus glucose uptake. (**b**) After a simple centrifugation step to remove cell pellets, the medium could be used directly for dehydration to generated acrylic acid. The reaction condition was the same with previously research[14], using TiO_2 as a catalyst at 230 °C for dehydration.

Supplementary Files

This is a list of supplementary files associated with this preprint. Click to download.

- TableS1SummaryofAcronym.xlsx
- TableS2StrainandPlasmidlist.xlsx
- TableS3DNAfragmentlist.xlsx
- Supplementaryfigure.docx